SRNS-STI-2010-00244

THERMAL ANALYSIS OF GEOLOGIC HIGH-LEVEL RADIOACTIVE WASTE PACKAGES

S. Y. Lee
Savannah River National Laboratory
Savannah River Site
Aiken, SC 29808
Phone: (803) 725-8462
si.lee@srnl.doe.gov

S. J. Hensel
Savannah River National Laboratory
Savannah River Site
Aiken, SC 29808
(803) 725-8440
steve.hensel@srnl.doe.gov

C. De Bock
ONDAF/NIRAS
Belgium
c.debock@nirond.be

ABSTRACT

The engineering design of disposal of the high level waste (HLW) packages in a geologic repository requires a thermal analysis to provide the temperature history of the packages. Calculated temperatures are used to demonstrate compliance with criteria for waste acceptance into the geologic disposal gallery system and as input to assess the transient thermal characteristics of the vitrified HLW Package.

The objective of the work was to evaluate the thermal performance of the supercontainer containing the vitrified HLW in a non-backfilled and unventilated underground disposal gallery. In order to achieve the objective, transient computational models for a geologic vitrified HLW package were developed by using a computational fluid dynamics method, and calculations for the HLW disposal gallery of the current Belgian geological repository reference design were performed. An initial two-dimensional model was used to conduct some parametric sensitivity studies to better understand the geologic system's thermal response. The effect of heat decay, number of co-disposed supercontainers, domain size, humidity, thermal conductivity and thermal emissivity were studied. Later, a more accurate three-dimensional model was developed by considering the conduction-convection cooling mechanism coupled with radiation, and the effect of the number of supercontainers (3, 4 and 8) was studied in more detail, as well as a bounding case with zero heat flux at both ends. The modeling methodology and results of the sensitivity studies will be presented.

Keywords: Geologic Repository, Supercontainer, Computational Heat Transfer, Computational Fluid Dynamics, Thermal Performance

INTRODUCTION

The Belgian National Agency for Radioactive Waste and Enriched Fissile Material, ONDRAF/NIRAS ((Organisme National des Déchets Radioactifs et des matières Fissiles enrichies (ONDRAF) /Nationale Instelling voor Radioactief Afval en verrijkte Splijtstoffen (NIRAS)), requested a statement of work for a transient thermal analysis of a proposed high level waste (HLW) disposal gallery [1,2]. The scenario to be analyzed is a no ventilation operating condition for the gallery region, which is not filled with a back-fill material. The analysis will address the transient temperature response of the supercontainer external surface, its internal waste package overpack, the air space, the wedge blocks, and the surrounding soil region.

The primary goal of the work is to develop a thermal model to simulate the thermal performance of the vitrified radioactive waste package in a HLW package disposal gallery during its operational phase, in order to evaluate the performance of the waste package from the thermal response under conservative operating conditions and to investigate the impact of certain parameters. The disposal gallery to be simulated is a 3 m inside diameter horizontal drift of 1000 m long, lined with concrete wedge blocks and located at a depth of several hundred meters, in the middle of a layer of poorly-indurated clay (Boom Clay formation). This disposal gallery contains the HLW in the form of supercontainers. Each supercontainer is a cylindrically-shaped structure weighing about 30 tons and consisting of two 180 liter canisters of vitrified HLW packed within a watertight carbon steel overpack embedded within a concrete shell. Each canister contains the heat source generated as result of a radioactive decay process of the vitrified HLW log.

As shown in Fig. 1, there is a void region, which is occupied by air and is assumed to be unventilated for the modeling calculations although it is in a later stage filled with grout material. Detailed geometrical dimensions for the repository configurations located inside the Boom Clay zone are presented in the figure.

Based on the modeling geometry as shown in Fig. 1, transient models were developed to accomplish the objective. The objective is to quantify the thermal response time of the supercontainer package to reach a certain temperature limit for a series of conservative operating conditions. Each supercontainer has the decay heat sources generated by the

vitrified HLW. In this work, the initial conditions of the supercontainer package is established by the steady-state calculations for the heat source corresponding to its residence time in an interim storage facility on the ground surface prior to being stored in a geologic repository such as the gallery tunnel.

A series of modeling calculations are performed here to estimate the thermal response time of the waste package under unventilated operating conditions in the gallery tunnel. The performance model is verified by the calculation results done by two different codes of MSC Patran [3] and FLUENT [4]. The verified model will be applied to the investigation of the thermal response of the package for different operating conditions and to the quantification of parametric sensitivities on thermal performance when the gallery region is not ventilated. This report will discuss the modeling and test results.

Although the initial thermal evaluations are limited to a two-dimensional (2-D) approach, more detailed three-dimensional (3-D) models are developed as a second phase work to evaluate the end effects of the waste form and to quantify the transient thermal response to the HLW packages in a geologic repository. A three-dimensional model of one or more waste units is analyzed here and transient results are compared with the initial 2-D model.

A series of sensitivity calculations for key paramters was also performed to examine the impact of the peak component surface temperatures due to change of design and operating parameters in a geologic repository. This paper discusses the modeling and analysis results.

NOMENCLATURE

A_W	Wall surface area (m^2)
°C	Degree Centigrade (or Celsius)
C	Constant for volumetric heat source
C_p	Specific heat (J/kg-K)
D	Diameter (m)
hr	Hour
k	Thermal conductivity (W/m-K)
L	Length (m) or latent of heat (cal/g)
LHS	Left hand side
m	Meter
mm	millimeter
min	Minute
OD	Outer diameter
q_{HLW}'''	Volumetric heat source for the HLW canister package (W/m^3)
q_W''	Wall heat flux (W/m^2)
Q	Power (watts)
RHS	Right hand side
r	Geometrical radius (m)
s or sec	Second
t	Time (year or sec)
t_{air}	Air temperature (°C)
T	Temperature (K)
ΔT	Temperature difference (K)
tHM	Metric ton of heavy metal
x, y, z	Three coordinate system for the computational domain shown Fig. 1
V_{HLW}	Volume of high-level waste (m^3)
W or watts	Power unit (=J/sec)
ρ	Density (kg/m^3)
β	Volumetric coefficient of thermal expansion (K^{-1})
μ	Dynamic viscosity (kg/(m-sec))
ε	Surface emissivity

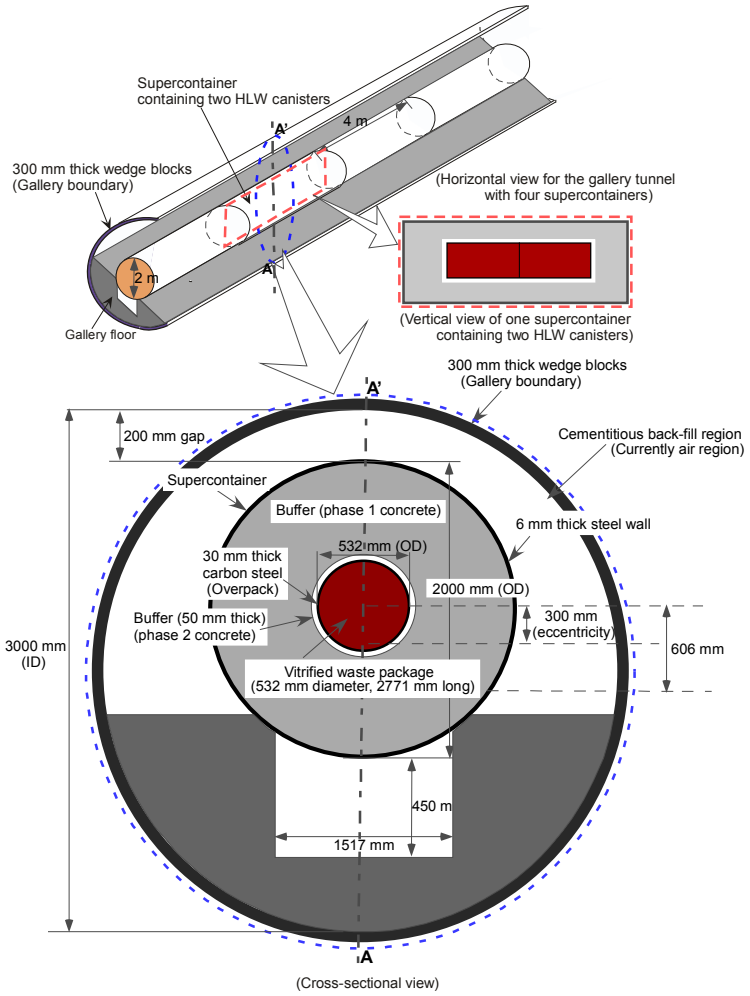

Figure 1. Two-dimensional modeling domain and geometry (Total length of the two canisters = 2771 mm).

MODELING APPROACH AND SOLUTION METHOD

The present work took a two-step modeling approach by using computational fluid dynamics (CFD) method for computational efficiency. As an initial approach, a two-dimensional conservative model was used to conduct some parametric sensitivity studies to better understand the geologic system's thermal response. The effect of heat decay, number of co-disposed supercontainers, domain size, humidity, thermal

conductivity and thermal emissivity were studied. As a final phase of the thermal performance analysis, a more accurate 3-D model was developed by considering the conduction-convection cooling mechanism coupled with radiation, and the effect of the number of supercontainers (3, 4 and 8) was studied in more detail, as well as a bounding case with zero heat flux at both ends.

Under the simple 2-D approach, two basic models are used to investigate what are the primary cooling mechanisms for the multi-layered and enclosed HLW package containing the decay heat sources in an unventilated geologic repository as shown in Fig. 1. One is the conduction-radiation model for the conservative estimate, and the other is the conduction-radiation coupled with convection for the best estimate. From these two models, the conservatism embedded in the first model can be quantified, if necessary. In addition, the first model provides the solutions more quickly than the second one does since the first method just solves the energy balance equations over the entire modeling domain without considering the momentum balance for the back-filled zone.

The modeling domain considered here includes the supercontainer, the gallery tunnel, and the soil region. Each supercontainer includes two vitrified HLW canisters, which have decay heat sources. The decay heat will be eventually dissipated through the soil medium since it is surrounded by the soil region. A series of the initial calculations were performed by using the conduction-radiation model for the modeling domains of 30m to 100m radius, assuming that the supercontainer is located at the center of the modeling domain. The results show that the temperature distributions are not sensitive to the domain size when the domain size is larger than 30m as shown later. For thermal analysis, the present calculations were performed for the 50m modeling domain size to include a clay domain.

Two different computer codes were used for the verification of the modeling calculations under the same initial and boundary conditions. The first MSC/Thermal (referred to as Thermal) uses network node resistance approach and solves conduction-radiation equations. Convection heat transfer is included via correlations or predetermined heat transfer coefficients. The second code is FLUENT which is a full Navier-Stokes based equation solver via the CFD method. Steady-State solutions were first obtained using both computer codes and different clay domain sizes. The Thermal results were used for the verification of the FLUENT modeling calculations, which were performed for all the analyses in this paper. The calculations for the two codes were performed under the conduction-radiation model, which is based on the conservative temperature estimate. These temperatures provide an upper bound to the problem and give proper modeling independent verification.

The solution methodology established in the 2-D modeling analysis was employed to determine the detailed 3-D transient temperature response of the system to the high-level waste (HLW) decay heat source. All the transient analyses were run until maximum temperatures for the supercontainer components were reached. In this work, two temperature limits were used for the waste package criterion in the geologic gallery repository. One is a critical temperature limit to prevent damage to the concrete buffers, which is the 100^{o}C external surface temperature limit of the overpack containing the heat source. The other is used as a guideline, which is the 60^{o}C temperature limit of the supercontainer surface. This will impact the air temperature to which repository personnel may be exposed.

The present calculations are based on the following assumptions:

- The heat dissipation along the horizontal direction of the supercontainer is assumed to be negligible since the work is based on a two-dimensional approach as shown in Fig. 1.
- The gallery region is unventilated for the evaluation.
- Free convection for the gallery region is governed by laminar flow regime since Rayleigh number (Ra) based on the vertical length scale of the supercontainer is typically less than 10^{10} [6]. This approach also provides a conservative estimate of thermal performance for the HLW package in the gallery repository.
- Heat source decay is uniformly distributed over the vitrified HLW canister.
- Material and thermal properties for all solid components are independent of temperature since the temperature range of the current analysis is expected to be from about 16^{o}C to a maximum 170^{o}C.
- Air humidity is assumed to be 50% relative humidity as requested by the client.
- Air follows an ideal gas behavior.
- The convection was assumed to be driven by the temperature gradient only since the gallery is unventilated.
- The reference value for radiation emissivity of the stainless steel is 0.2 for conservatism (highly polished steel). This assumes that fouling for the stainless steel surface of supercontainer during the geologic storage is negligible.
- The supercontainer is located at the center of the modeling domain.

Complete setup of the modeling calculations requires the input parameters such as thermal and material properties of the package components, heat source term, initial and boundary conditions, and domain discretization, along with the established modeling domain and assumptions. They will be discussed in subsequent sections.

The transient heat source was based on the assumption that the heat source is uniformly distributed throughout the entire volumes of two HLW canisters (2.711 m long). The heat source region is indicated as the red zone in Fig. 1. For the modeling calculations, volumetric heat generation rate for the

canister regions was used as heat source input to the transient model.

The decay heat curve provided by the client was based on Category C radioactive waste heat source [1,2]. The transient decay curve for a single canister was converted into transient volumetric heat source per each supercontainer q_{HLW}''' for the calculations. It is given by Eq. (1) in terms of transient time, t years, considering that each supercontainer contains two canisters. The volumetric heat source q_{HLW}''' is in watts per m^3.

$$q'''_{HLW}(t) = CQ = C\left\{0.1 + 5021e^{-\lambda_1(t+60)} + 1205e^{-\lambda_2(t+60)} + 27.04e^{-\lambda_3(t+60)} + 0.7576e^{-\lambda_4(t+60)}\right\} \quad (1)$$

Two different heat sources were modeled for the two-dimensional thermal calculations. One is the baseline case, the most conservative approach. It is based on the assumption that the HLW canister containing the heat source is infinitely long under the two-dimensional modeling domain as shown in Fig. 1. The other case is based on the assumption that heat source is uniformly distributed through the 4-m supercontainer along the horizontal direction of the gallery tunnel.

The constant, *C*, in Eq. (1) has two values, depending on the source modeling cases under the present two-dimensional approach. When each supercontainer has 2.66 tHM (ton of Heavy Metal) content corresponding to two canisters, they are C = 5.6076 for the baseline volumetric source and C = 3.8006 for the homogenized volumetric source. The coefficients in Eq. (1) are as follows:

$$\begin{aligned} \lambda_1 &= 3.894 \times 10^{-1} \\ \lambda_2 &= 2.458 \times 10^{-2} \\ \lambda_3 &= 1.630 \times 10^{-3} \\ \lambda_4 &= 6.546 \times 10^{-5} \end{aligned} \quad (2)$$

As shown in Eq. (1), it should be emphasized that the present calculations used the 60-year old supercontainer as the initial heat source in a geologic repository. Based on the decay curve of Fig. 2, the heat source contained in the supercontainer was estimated during the early period of the gallery storage as shown in Table 2. The results shown in the table indicate that the heat source is reduced by about 11% within the first five-year period.

Volumetric heat generation rate was used for the vitrified canister region as heat source input to the transient calculations. Based on Eq. (1), the transient volumetric heat source is shown as a function of geologic storage time in Fig. 2. It is noted that the volumetric heat source is initially 1688.5 watts/m^3, corresponding to the thermal source of 801.0 watts for each supercontainer. This transient heat source was used for the present calculations.

The initial temperature distributions for the transient cases were determined by solving a steady-state solution of the supercontainer with a 40°C overpack container fixed temperature under the decay heat source as shown in Fig. 2. Air temperature was 20°C and gallery floor, wedge blocks, and clay were 15.7°C at the beginning of geologic gallery storage. In this case, the temperature distributions of the supercontainer region established under the steady state conditions were used as the initial conditions for the transient modeling calculations. Figure 3 compares the initial temperature distributions for the 50m modeling domain for the baseline and homogenized source cases with a 40°C supercontainer surface temperature. The results established for the initial temperature distributions over the 50m modeling domain are shown in Fig. 3.

For the modeling boundary conditions, a constant temperature of 15.7°C was imposed at the boundary of the 50m modeling domain. The modeling domain was discretized for the numerical calculations. Grid independent studies were performed to ensure appropriate mesh refinement was used. The overall energy balance should be checked to demonstrate the adequacy of the grid fineness used. This was done by using Eq. (7).

$$R = -\int_{A_W} q''_w dA + q_{HLW}'''(t) V_{HLW} \quad (7)$$

Volumetric heat source term, q_{HLW}''', in Eq. (7) is given by the code input. For all the cases considered here, energy residual (*R*) is less than about 0.5 watt. For the present analysis, the optimum grids of about 56,000 nodes for the 2-D analysis and about 1.5 to 3 million hexahedral meshes for the 3-D computational domain have been established from the grid sensitivity analysis under Linux high performance computer platform.

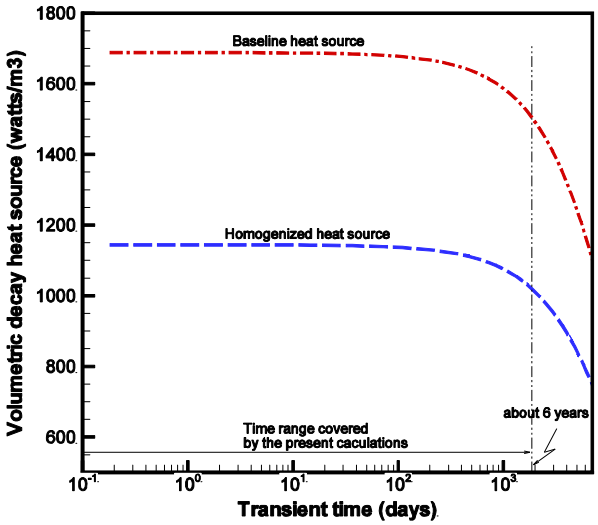

Figure 2. Transient volumetric heat sources as function of geologic storage time used for the present transient calculations (Initial heat source is 801.0 watts per supercontainer).

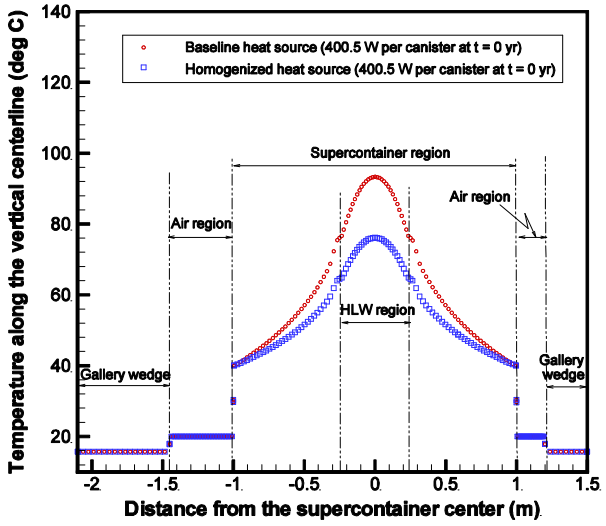

Figure 3. Initial temperature distributions along the vertical centerline of the supercontainer with 50m soil domain and 40°C supercontainer surface temperature, 20°C initial air temperature, and 15.7°C initial soil temperature.

Table 1. Reference thermal and material properties used for the modeling calculations

Material components	k (W/m-K)	ρ (kg/m^3)	C_p (J/kg-K)	ε
Boom Clay	k_{hor} = 1.7, k_{vert} = 1.25	2000	1450	NA
HLW	1.355*	2750	1089*	NA
Overpack wall (carbon steel)	54	7830	465	NA
Buffer (1st phase)	1.89	2420	1000	NA
Buffer (2nd phase)	1	2400	880	NA
Liner stainless steel	17	7850	500	0.2
Gallery lining^{++} (wedge block)	1.5	2400	750	0.8
Gallery floor	1.5	2400	750	0.8
Air***	Temp.-dependent**	Ideal gas	1006	NA$^+$

Note:*Values averaged at two different temperatures

** $k_{air} = 3.3350x10^{-3} + 8.0021x10^{-5}(273.15 + t_{air}) - 1.8975x10^{-8}(273.15 + t_{air})^2$, where t_{air} is in °C [5].

***For the baseline calculations, air was assumed to be zero humidity.

$^+$Assumed air to be non-participation medium

RESULTS AND DISCUSSIONS

The effect of heat decay, number of co-disposed supercontainers, domain size, humidity, thermal conductivity and thermal emissivity were studied by the 2-D model. Later, a more detailed 3-D model was developed by considering the conduction-convection cooling mechanism coupled with radiation, and the effect of the number of supercontainers on transient thermal responses was studied, as well as a bounding case with zero heat flux at both ends.

2-D Modeling Results

Based on the initial temperature distributions in Fig. 3 and 15.7°C soil boundary temperature, two basic transient models were developed by considering the conduction-radiation and the conduction-radiation coupled with convection, referred to as cond-rad and cond-rad-conv model in the text, respectively. For these models, two heat source approaches are considered for the 2-D modeling approach as discussed earlier. They are the baseline and the homogenized heat sources. Thermal performance calculations for each heat source were performed by both of the cond-rad and cond-rad-conv models. In the latter case, the convection was assumed to be driven by the temperature gradient only since all calculations were based on the unventilated gallery as one of the reference conditions.

The transient results for the baseline heat source indicate that the 60°C supercontainer temperature guideline is reached before the overpack reaches the 100°C limit. Figure 4 compares the transient maximum surface temperatures for the

overpack and the supercontainer between the two baseline models, cond-rad model and cond-rad-conv model. It is noted that the transient thermal response of the overpack surface to the HLW heat source is very slow due to the large thermal inertia of the buffer material adjacent to the overpack during early transient periods. In this case the ratio of thermal conductivity to thermal capacity, namely, product of density and thermal capacity, is referred to as thermal diffusivity, which is shown as a material constant in the transient term of the energy balance equation. Substances with low thermal diffusivity such as soil slowly adjust their temperature to that of their surroundings, because they conduct heat slowly in comparison to their volumetric heat capacity. For instance, thermal diffusivity of the buffer material adjacent to the HLW canister is about 0.8 mm^2/sec, compared to about 26 mm^2/sec of air. The impact of including natural convection is significant with the time to reach the 100°C temperature limit for the overpack surface being 93 days compared with only 54 days when natural convection is conservatively neglected. Table 2 compares the results between the two models. It is worth noting that a negligible amount of heat source decay occurs for such a short transient as shown in Fig. 2.

The transient results for the homogenized heat source case show that the supercontainer surface temperature reaches the 60°C temperature guideline much earlier than the overpack reaches the 100°C limit. As shown in Fig. 5, it takes about 6 years for the overpack surface to reach about 97°C peak temperature even using the conservative cond-rad model. The calculation results show that after reaching the peak temperature, the overpack surface temperature starts to decrease since the heat source at about 6 years' storage time is already reduced by about 12% from the initial value of 1144 watts/m^3. As shown in Fig. 5, the cond-rad-conv model predicts about 3°C lower than the cond-rad model does since natural convection provides an additional cooling mechanism from the gas circulation inside the gallery. Table 4 quantitatively compares times to reach the temperature limit for the baseline and homogenized heat sources. Although the homogenized heat source model is slightly non-conservative with respect to expected actual overpack temperatures, it is a more realistic 2-D approximation than the very conservative baseline model as shown in the 3-D results.

A parametric sensitivity evaluation was performed to investigate the impact of ambient humidity, material properties, and transient decay heat on the transient thermal performance of the HLW waste package when a disposal gallery is assumed to be unventilated. The sensitivity evaluation results for the key parameters considered here are presented in the Appendix. When the relative humidity of the gallery air increases from 0 to 50%, the modeling results show that the 50%RH air case takes about 10 hours longer than the dry air case in reaching the 100°C limit of max. overpack surface temperature because of the increased thermal capacity from the presence of the vapor species in the air medium. When the material and thermal properties of the package components such as the gallery lining and the soil are changed from the reference values to the literature data, the thermal response times to reach the 100°C temperature limit of the overpack surface are varied by about 10% with respect to the reference results.

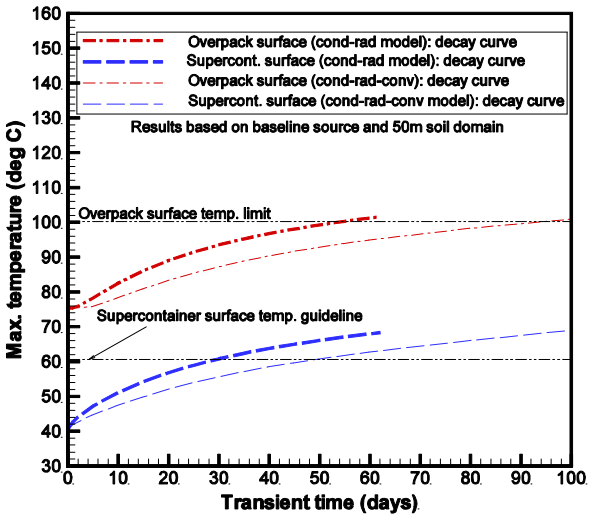

Figure 4. Transient max. surface temperatures for overpack and supercontainer between two different models with baseline decay heat source.

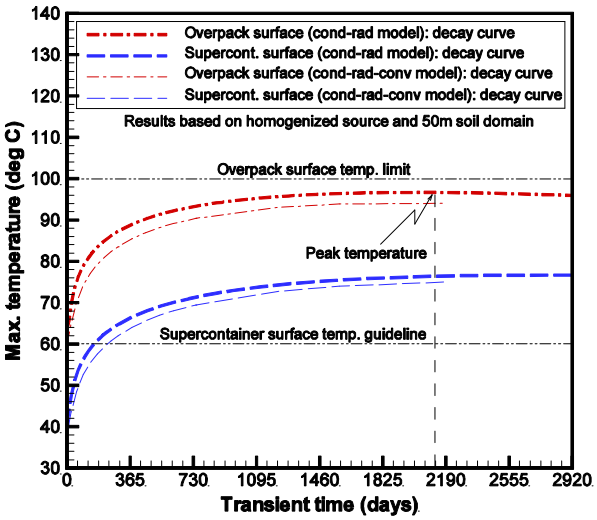

Figure 5. Transient max. surface temperatures for overpack and supercontainer between two different models with homogenized decay heat source.

The sensitivity evaluation shows that transient decay heat has the largest impact on the thermal response time after one

year residence time. The sensitivity results for the selected key parameters are summarized in Table 3.

Table 2. Comparison of times to reach temperature limit for the baseline and homogenized heat sources

Locations	cond-rad model		cond-rad-conv model	
	Baseline	Homogenized	Baseline	Homogenized
Overpack surface (100°C)	54 days	Never reaching 100°C (T_{max} = 97°C)	93 days	Never reaching 100°C (T_{max} < 97°C)
Super-container surface (60°C)	28 days	157 days	48 days	235 days

Table 3. Summary results for the key parameters considered for the sensitivity study

Sensitivity parameters	Parametric changes	Impact on thermal responses of the overpack surface
Soil domain size	30 to 50 m	Temperature response of package surface: about 1% faster
Air humidity	0 to 50%RH	Temperature response of package surface: about 1% slower
Surf. emissivity (supercont.)	0.2 to 0.8	About 9% max. temperature decreased
Soil (Boom Clay)	Thermal diffusivity changed from 0.51 to 0.72 mm^2/sec	Temperature response of package surface: about 10% faster
Gallery lining	Thermal diffusivity changed from 0.83 to 0.81 mm^2/sec	Temperature response of package surface: about 13% slower
Decay heat	About 7% source decreased due to power decay in about 3 years	Temperature response of package surface: about 17% slower

Detailed 3-D Modeling Results

The solution method verified by the initial 2-D modeling approach was applied to the 3-D thermal performance calculations for the transient heat source by using the cond-rad-conv model. In all cases, the convection was assumed to be driven only by the temperature gradient since all calculations were based on an unventilated gallery.

As shown in Table 4, five different cases were considered here, depending on the number of supercontainers stored in the gallery tunnel and the empty air space of the gallery for the given initial and soil boundary conditions. The modeling results for the cases are discussed here. The geometrical configurations and modeling boundaries for Case-1 are shown in Table 4. When both ends of the three supercontainers contacted in series were imposed by a zero heat flux boundary without any empty air space or back-filled region in the gallery tunnel, the transient results for the Case-1 model indicate that the 60°C supercontainer temperature guideline is reached before the overpack reaches the 100°C limit as shown in Fig. 6. Figure 6 shows the transient maximum surface temperatures for the overpack is 101°C and for the supercontainer is 74°C. The peak temperature was reached in about 5 years' storage period. Detailed temperature distributions for the vertical plane crossing the middle of the 2nd supercontainer at the time of peak temperatures are shown in Fig. 7. Temperature distributions of the overpack and supercontainer surfaces along the horizontal gallery tunnel are shown in Fig. 8. Figure 9 presents the oscillating distributions of the surface temperatures along the horizontal gallery tunnel at the storage time of 4.5 years. In this case, the heat sink at both side ends of the first and the last supercontainers was not considered as shown in Table 3.

Air temperature distributions for the vertical back-filled region of the gallery tunnel crossing the middle of the horizontal supercontainer at the time of peak temperature are shown in Fig. 7. Flow patterns for the gallery air region are shown in Fig. 10. Figure 11 shows oscillatory air velocity profiles for the top air space of the gallery tunnel due to non-uniform heat source along the horizontal gallery tunnel. When the supercontainers reach peak temperature during the storage period, the temperature contours along the central vertical plane of the gallery tunnel are presented in Fig. 12. As shown in Table 1, the surface emissivity for the supercontainer was assumed to be 0.2 as one of the reference conditions. When the emissivity increases from 0.2 for a shiny surface to 0.3 for a smooth surface, the results show that the maximum surface temperature decreases by about 2°C (T_{max}=99°C).

The modeling domain for Case-2 includes a 4m unventilated air space at the left-hand side and a 4m back-filled concrete region at the right-hand side of the three supercontainers as shown in Table 3. The results of Case-2 indicated that the transient thermal response of the overpack surface to the HLW heat source is slower than Case-1. The larger heat sink supplied by the soil surrounding the gallery in Case-2 versus Case-1 allowed for significant heat flow to the left and right sides of the heat source. The total heat transfer rate to the heat sink is also increased, thus, reducing the rate of temperature increase at the overpack surface and resulting in about 12°C lower maximum temperature. Because Case-2 has a 4m cement region at one end of the three supercontainers in the gallery and a 4m air layer at the other end, the temperature gradients at their interfaces are very steep due to conduction, convection, and radiation cooling mechanisms instead of the insulation boundaries of Case-1. Figure 13 shows the temperature distributions for various locations of the supercontainer components containing three supercontainers

along the horizontal gallery drift tunnel at the transient time of about 3.8 years.

The modeling results shown in Fig. 13 indicate that hot air always stays near the top wedge inner surface because of its buoyancy. It is noted that the top wedge inner surface temperature for the additional 4m air space increases from the initial temperature of 15.7°C up to about 42°C in about 4 years' residence time. These results indicate that the surrounding structural materials such as wedge blocks and soil provide a significant conduit of heat flow to remove the decay heat from the supercontainer region to the 4m empty gallery region. To illustrate the effect of the surrounding structural materials further, an increase in the length of empty gallery from 4 m (Case-2) to 16m (Case-3) results in a decrease of the air temperature in the empty region of about 10°C as shown in Fig. 14. These result clearly indicate an increased dissipation of heat along the empty gallery. Thus, substances with low thermal diffusivity such as soil slowly adjust their temperature to that of their surroundings, because they conduct heat slowly in comparison to their volumetric heat capacity.

The modeling results for Case-4 show that the overpack surface temperature is about 2°C higher than for Case-3 since the number of supercontainers increases for the length of the empty gallery considered as part of modeling domain. It is noted that the maximum overpack surface temperatures for these two cases do not exceed 90°C.

The modeling results show that the peak surface temperature of the overpack for the bounding Case-1 modeling conditions is 101°C, which is the highest temperature among all the cases including Case-5 since both side ends of the waste packages are imposed by the zero heat sink boundaries. When eight supercontainers are contacted in series with one of their side ends exposed to a 16m air space and the other is imposed with a zero heat flux boundary, the peak temperature of the overpack surface is 90.8°C. This temperature is reached by the supercontainer closest to the zero heat flux end. All the other overpacks are at gradually lower temperatures towards the air space on the LHS. This is a conservative analysis because a zero heat flux was imposed on the RHS.

When the number of supercontainers stored in the gallery is increased from 3 to 8 under the same storage boundary conditions, the supercontainer surface temperature increases with more supercontainers stored in the gallery repository. Figure 15 presents the oscillating distributions of the surface temperatures along the horizontal gallery tunnel at the peak temperature time of 3.6 years' storage. The figure also compares the temperature distributions for key components of the supercontainer packages under the same boundary conditions of three storage cases, Case-3 to Case-5.

The peak overpack surface temperatures for different numbers of supercontainer storages are compared in Fig.16 under the same boundary conditions at 1.6 years and at 3.6 years (time to peak temperature). The Figure also shows the bounding Case-1 peak temperature. Table 5 provides a quantitative comparison of the times to reach the temperature limits for all five cases, or the maximum temperatures reached if lower than the limits. As shown in the table, the transient results for the Case-5 model indicate that the 60°C supercontainer temperature guideline is reached in about 1.2 years and a maximum temperature of 65°C is eventually reached. It should be noted that the peak surface temperature of the overpack in the supercontainer cannot be higher than 101°C for the boundary conditions studied, and that the Case-1 storage conditions provides the most conservative estimate. The calculation results show that the results of the simple 2-D homogenized model are about 6% higher than the 3-D modeling results of Case-5 in terms of maximum package temperature.

CONCLUSION

Transient computational models were developed for a High-Level Waste (HLW) disposal gallery in non-backfilled and unventilated conditions. Primary objective was to evaluate the transient thermal characteristics and to perform some parametric sensitivity studies inside the gallery tunnel.

Two modeling calculations for 2-D sensitivity calculations and 3-D performance analysis were performed to achieve the objective of the work. The 2-D modeling results were used for establishment of solution method and sensitivity evaluations of key design and operating parameters such as domain size and decay heat source. Detailed 3-D computational calculations were made for the evaluation of thermal performance under five different HLW storage configurations by considering the number of the supercontainers stored in the gallery and the size of the empty gallery space. Based on the initial temperature distributions in Fig. 3, the thermal performance calculations for each case were performed by the conduction-radiation-convection mechanism. In all cases, convection was considered to be driven by the temperature gradient only since all calculations were based on the unventilated gallery. In this work, a 100°C external surface temperature of the overpack was used as the temperature limit for the geologic gallery repository, and a 60°C guideline was used for the supercontainer surface temperature.

The main results are summarized as follows:

- The impact of empty gallery air space is significant under time-dependent decay heat: The 100°C overpack temperature limit is never reached under the partially loaded gallery as summarized in Table 5. The results demonstrate that the HLW disposal system is safe with respect to the 100°C limit as shown in the table for the peak temperature values. Only in the bounding case, Case-

1, maximum temperature on the overpack surface exceeds the limit by 1°C. In Case-5, which has the highest thermal load configurations currently considered for the operation, the peak temperature stays well below the limit. In any case, the maximum overpack temperature is reached only after three years into the transient, leaving a plenty of time duration for a potential intervention. In addition, although there is likelihood to exceed the 60°C guideline under certain circumstances, this would only have an impact on operational aspects, but it is not directly related to safety.

- The modeling results clearly indicate that even for an unventilated gallery, free convective flow patterns are generated by non-uniform heat source along the horizontal gallery tunnel as shown in Fig. 11.
- The impact of the increased thermal loads on the thermal performance of supercontainer is important: Less than 2°C increase for one additional supercontainer (from 3 to 4 supercontainers).
- Sensitivity analysis for the radiation emissivity of the supercontainer surface was performed. The results show that when the emissivity increases from 0.2 for a shiny surface to 0.3 for a smooth surface, the maximum surface temperature decreases by about 2°C. The temperature decrease would be even more significant for a corroded surface.
- The sensitivity results indicate that when the length of empty gallery becomes larger, the transient thermal response to the supercontainer loadings is significantly slower. This effect results from the increased heat sink region corresponding to the length of empty gallery considered in the model. For instance, when the length of empty gallery is increased from 0 to 16m, the maximum overpack surface temperature is decreased by about 17°C, assuming that the supercontainer is located at the center of the modeling domain.
- The modeling results show that the simple 2-D homogenized model provides higher maximum package temperatures than the 3-D model (by 6% for Case-5)

ACKNOWLEDGMENT

This manuscript has been authored by Savannah River Nuclear Solutions, LLC under Contract No. DE-AC09-08SR22470 with the U.S. Department of Energy. The United States Government retains and the publisher, by accepting this article for publication, acknowledges that the United States Government retains a non-exclusive, paid-up, irrevocable, worldwide license to publish or reproduce the published form of this work, or allow others to do so, for United States Government purposes.

REFERENCES

1. Chris De Bock's E-mail attachment forwarded by E. Raskin, March 4, 2009
2. S. Y. Lee and N. K. Gupta, "Two-dimensional Thermal Performance Analysis for HLW Disposal Gallery", SRNL technical report, WFO-08-014, May 14, 2009.
3. MSC.Patran/Thermal, Version 2003 Rev. 2, Online Manual, MSC.Software Corporation, Santa Ana, California, 2003
4. FLUENT, 2008, Fluent, Inc., Lebanon, New Hampshire.
5. S. E. Aleman, G. P. Flach, L. L. Hamm, S. Y. Lee, and F. G. Smith, III, 1993, "FLOWTRAN-TF Code Software Design (U)", WSRC-TR-92-532, Savannah River National Laboratory, Westinghouse Savannah River Company, February 1993.
6. W. M. Kays and M. E. Crawford, *Convective Heat and Mass Transfer*, Second Edition, McGraw-Hill Book Company, New York (1980).

Table 4. Five different cases considered for the three-dimensional transient calculations

Cases	Number of supercontainers stored in the gallery	Air space at LHS of the far-left supercontainer	Space at RHS of the far-right supercontainer
Case-1	3	None (zero wall heat flux boundary)	None (zero wall heat flux boundary)
Case-2	3	4 m long	4 m long (filled with cement)
Case-3	3	16 m long	None (zero wall heat flux boundary)
Case-4	4	16 m long	None (zero wall heat flux boundary)
Case-5	8	16 m long	None (zero wall heat flux boundary)

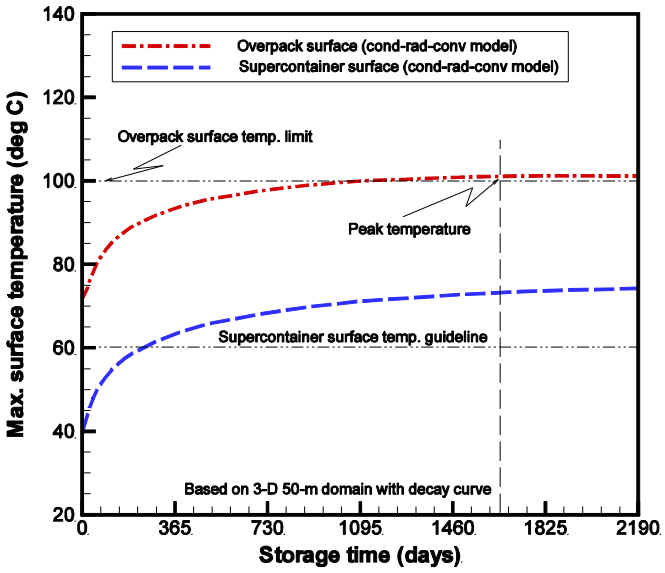

Figure 6. Transient maximum temperatures for overpack and supercontainer surfaces for Case-1

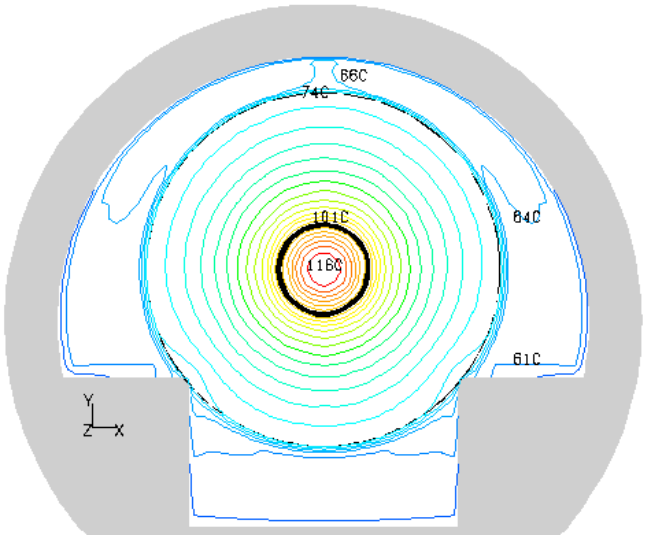

Figure 7. Temperature distributions for the Case-1 model for the vertical cross-sectional plane crossing the middle of the horizontal supercontainer after 4.5 years' storage

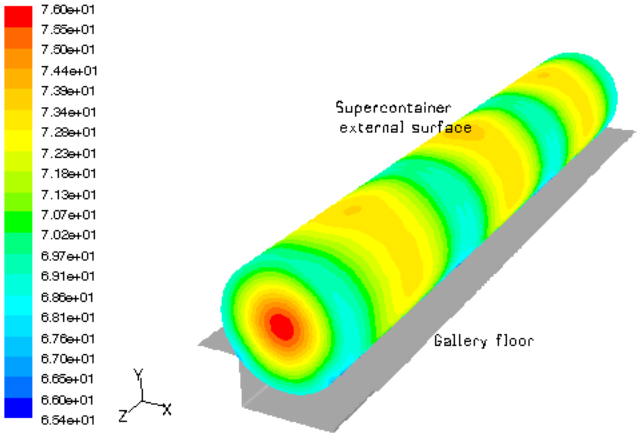

(Supercontainer surface temperatures)

Figure 8. Temperature distributions for supercontainer surfaces for the Case-1 (3 supercontainers) at t ≈ 4.5 years

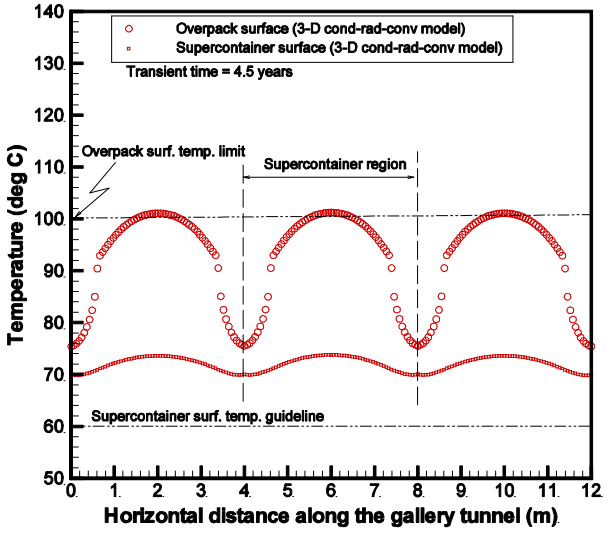

Figure 9. Temperature distributions at 4.5 storage years along the horizontal gallery tunnel

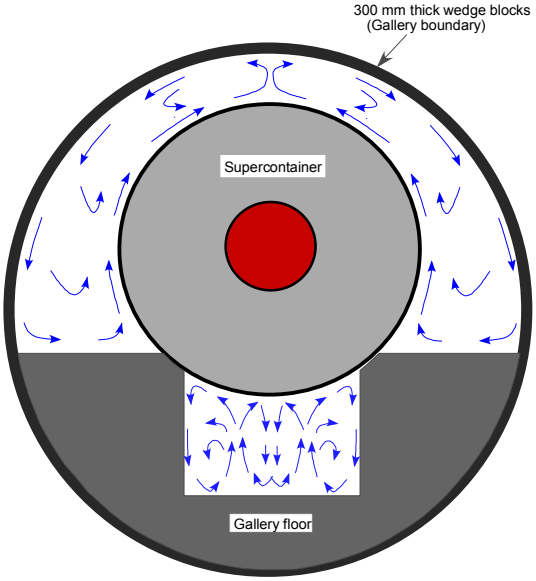

Figure 10. Overall air flow patterns due to natural convection for the back-filled region of the gallery tunnel crossing the middle of the horizontal supercontainer after about 5 years' storage

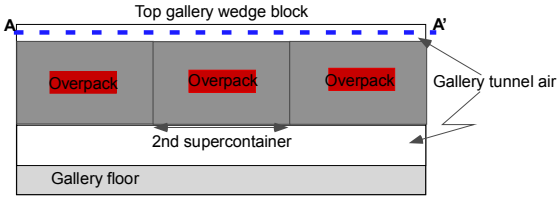

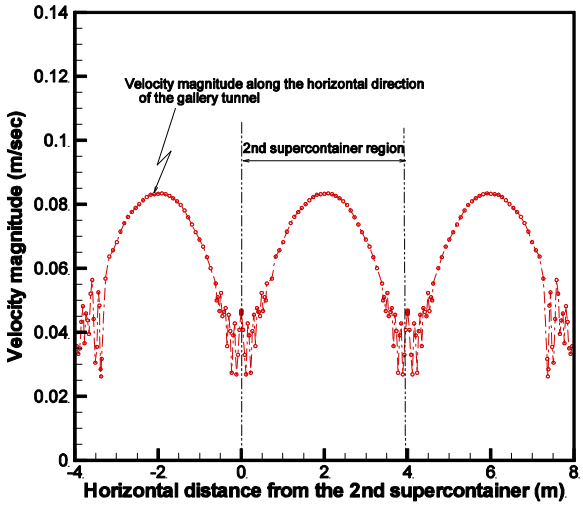

Figure 11. Air velocity profiles along the line A-A' for the top air space of the gallery tunnel at about 5 storage years

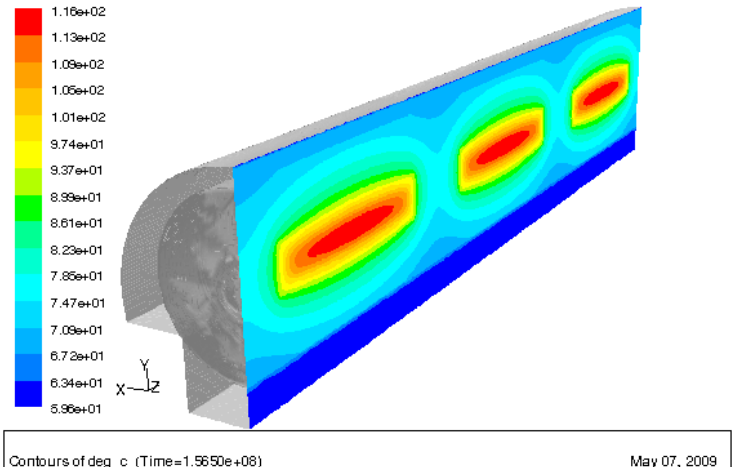

Figure 12. Temperature contours at about 5 storage years along the central vertical plane of the gallery tunnel for Case-1 (Numbers in the color code are in ^{o}C)

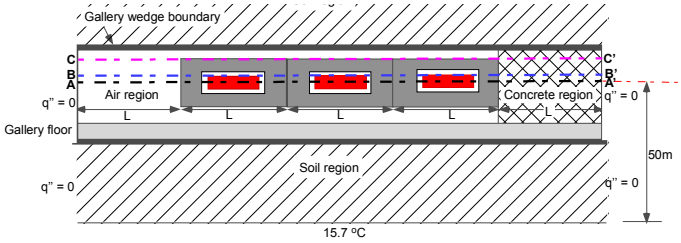

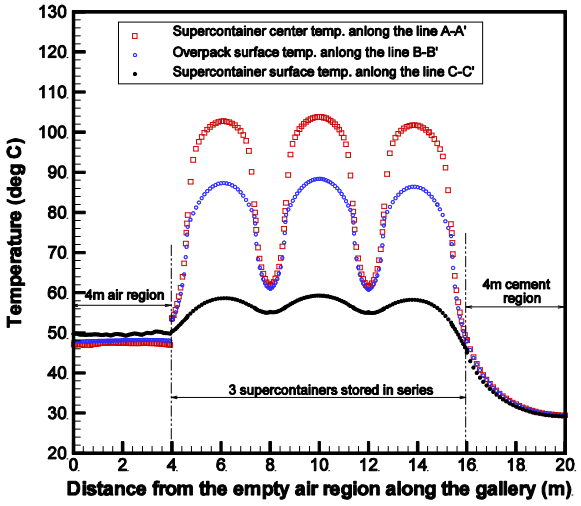

Figure 13. Temperature distributions along the lines, A-A', B-B', C-C', for the supercontainer components for the gallery tunnel containing three supercontainers along the horizontal gallery drift tunnel after about 4 years (Case-2)

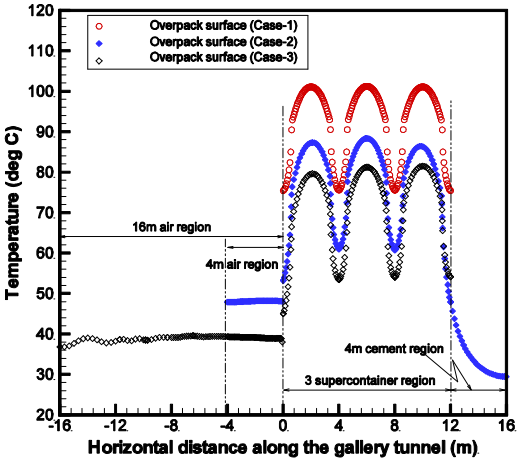

Figure 14. Comparison of temperature distributions along the top overpack surface for three supercontainers stored inside the gallery tunnel after about 4 years

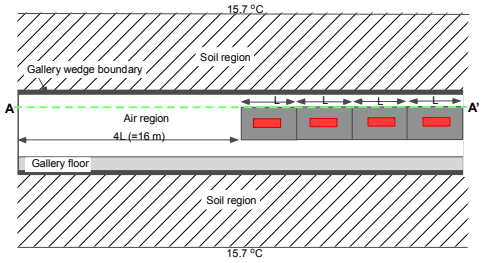

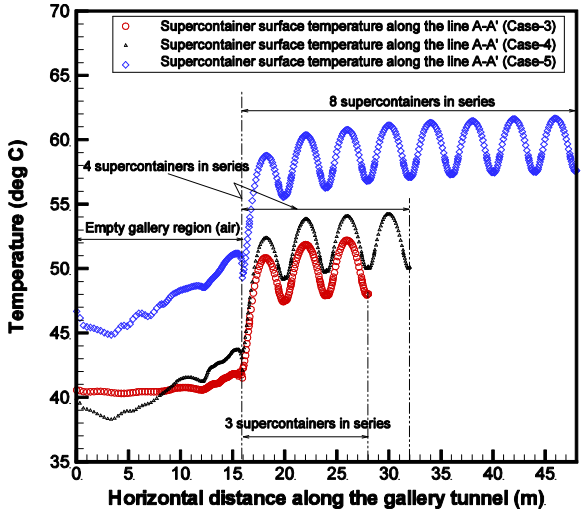

Figure 15. Comparison of supercontainer surface temperature distributions for different numbers of supercontainer storages with 16m empty air space on LHS end and insulation boundary at RHS end.

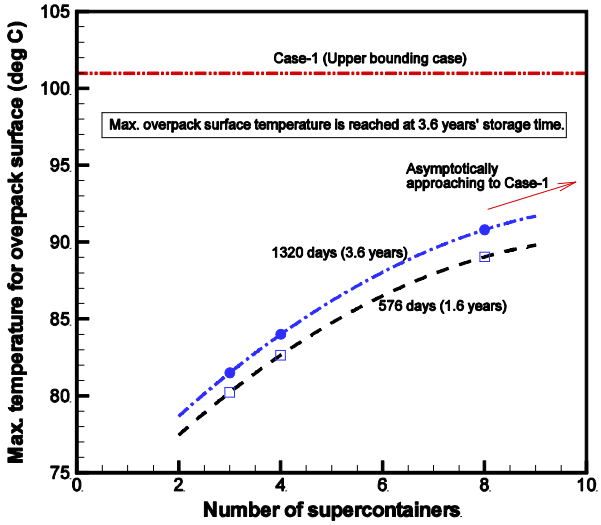

Figure 16. Peak overpack surface temperatures for different numbers of supercontainer storages with 16m empty air space on LHS end and insulation boundary at RHS end at various storage times

Table 5. Comparison of times to reach temperature limit for the two- and three-dimensional models

Package components surface			Overpack surface (100°C)	Supercont. Surface (60°C)
Models	2-D model		Never reaching 100°C (T_{max} < 97°C)	235 days (T_{max} = 76°C)
	3-D model	Case -1	3.1 yrs (T_{max} = 101°C for the entire storage period)	241 days (T_{max} = 74°C)
		Case-2	T_{max} < 89°C for the entire storage period	2.2 yrs T_{max} = 62°C for the entire storage period
		Case-3	T_{max} < 82°C for the entire storage period	T_{max} < 55°C for the entire storage period
		Case-4	T_{max} < 84°C for the entire storage period	T_{max} < 58°C for the entire storage period
		Case-5	T_{max} < 91°C for the entire storage period	1.2 years T_{max} = 65°C during the entire storage period